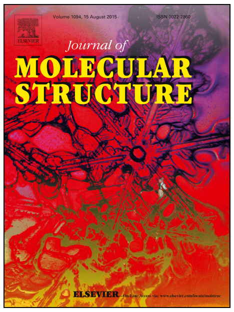

Synthesis, Structural characterization, thermal, molecular modeling and biological studies of chalcone and Cr(III), Mn(II), Cu(II) Zn(II) and Cd(II) chelates

Tarek A. Fayed, M. Gaber, Marwa El-Nahass, H.A. Diab, Mohammed M. El-Gamil

PII: S0022-2860(20)31067-X

DOI: https://doi.org/10.1016/j.molstruc.2020.128742

Reference: MOLSTR 128742

To appear in: *Journal of Molecular Structure*

Received Date: 17 March 2020

Revised Date: 15 June 2020

Accepted Date: 22 June 2020

Please cite this article as: T.A. Fayed, M. Gaber, M. El-Nahass, H.A. Diab, M.M. El-Gamil, Synthesis, Structural characterization, thermal, molecular modeling and biological studies of chalcone and Cr(III), Mn(II), Cu(II) Zn(II) and Cd(II) chelates, *Journal of Molecular Structure* (2020), doi: https://doi.org/10.1016/j.molstruc.2020.128742.

Credit Author Statement

1. **Tarek. A. Fayed, Professor of Physical Chemistry, Chemistry Department, Faculty of Science, Tanta University, Egypt. His research interests include the design of optical chemical sensors for selective discrimination of toxic metal ions.**
2. **M.Gaber, Professor of Inorganic Chemistry, Chemistry Department, Faculty of Science, Tanta University, Egypt. His research interests include synthesis and characterization of ligands and their metal complexes.**

3. **Marwa N. El-Nahass, Associate Professor of Physical Chemistry, Chemistry Department, Faculty of Science, Tanta University, Egypt. Her interests include the design of chemosensors for optically selective, sensing and colorimetric detections of pollutants for environmental cleanup of toxic heavy metal ions.**

4. **H. A. Diab, Ph.D student, Chemistry Department, Faculty of Science, Tanta University, Egypt**

5. **Mohammed M. El-Gamil, recieved his Ph.D from Chemistry Department. Faculty of Science, Tanta University, Egypt. He works at Department of Toxic and Narcotic Drug, Forensic Medicine, Mansoura Laboratory, Medico legal Organization, Ministry of Justice, Egypt.**

Synthesis, Structural characterization, thermal, molecular modeling and biological studies of chalcone and Cr(III), Mn(II), Cu(II) Zn(II) and Cd(II) chelates

Tarek A. Fayed[*a], M. Gaber[*,a], Marwa. El-Nahass[a], H. A. Diab[a], Mohammed M. El-Gamil[b]

[a]Department of Chemistry, Faculty of Science, Tanta University, 31527, Tanta, Egypt.

[b]Department of Toxic and Narcotic Drug, Forensic Medicine, Mansoura Laboratory, Medico legal Organization, Ministry of Justice, Egypt.

Abstract:

A number of new Cr(III), Mn(II), Cu(II) Zn(II) and Cd(II) chelates of (E)-3-(4-(dimethyl-amino)phenyl)-1-(pyridin-2-yl)prop-2-en-1-one were synthesized. The structures were elucidated by elemental and thermal analysis as well as spectral techniques (mass, IR, and electronic spectra) and magnetic measurements. The IR data suggested that the investigated chalcone acted as a bidentate ligand via the O and N atoms of the C=O and C=N groups, respectively. The spectral plus magnetic data revealed the formation of octahedral structures for all chelates while Cu(II) chelate has the square planar geometry.The kinetic and thermodynamic parameters of the thermal decomposition stages have been evaluated. Molecular orbital calculations have been performed to confirm the geometry of the isolated compounds. The *in vitro* antimicrobial activities of the chalcone and its metal chelates have been performed against some bacterial strains. The data indicated that all the metal chelates demonstrated a higher activity than the free chalcone. The anticancer activity of the mentioned metal chelates is evaluated against MCF7 cell. These compounds exhibited a moderate and weak activity against the tested cell line. The results were correlated with the experimental data.

Keywords: Chalcone; Metal chelates; Thermal behavior; Antimicrobial, Molecular modeling, Anticancer.

---

* E-mail: mabuelazm@science.tanta.edu.eg, tfayed2013@science.tanta.edu.eg, marwa.elnahas@science.tanta.edu.eg.

1. Introduction

Chalcones are a class of flavonoid natural products consisting of two aryl rings linked by α,β-unsaturated ketone moiety. Chalcones have proved to be versatile extensive applications in wide ranging of biological area such as antimalarial, antibacterial, antitumor, antioxidant, anti-inflammatory,antihyperglycemic,and anti-HIV [1-8]. This class of compounds had been extensively used as fluorescent probes for metal ions detection [9-11] or DNA [12]. Chalcone compounds played animportant role in the development of coordination chemistry, as they readily form stable chelates with most transition metals.Thus, the chalcone metal chelates and related compounds have been studied, due to their interesting behavior in catalytic and biological applications [13-22].

In continuation to our research which aimed at synthesis and characterization of chalcones and their chelates [23-27], Cr(III), Mn(II), Cu(II), Zn(II) and Cd(II) chelates of chalcone compound namely, (E)-3-(4-(dimethylamino)phenyl)-1-(pyridin-2-yl)prop-2-en-1-one (Structure 1) have been prepared. The synthesized chalcone and its metal chelates have been characterized by different techniques like elemental analyses, spectral studies, TGA, magnetic and conductance measurements. In vitro antimicrobial and anticancer activities of the free chalcone and its metal chelates involved in this study have also been assessed. Molecular orbital calculations have been performed for the investigated metal chelates.

2. Experimental

2.1. Materials

All compounds used in the present study were of pure grade available from BDH, Aldrich or Sigma. The metal salts, $Mn(CH_3COO)_2.4H_2O$, $Cr_2(CH_3COO)_4(H_2O)_2$, $Cd(CH_3COO)_2$, $Cu(NO_3).3H_2O$, $Zn(CH_3COO)_2.2H_2O$, and $ZnCl_2$ were used. The solvents used for the spectral study were spectroscopic grade from Aldrich.

Section 2.2. Preparation of solid compounds

The titled chalcone, (E)-3-(4-(dimethylamino)phenyl)-1-(pyridin-2-yl)prop-2-en-1-one structure was prepared and characterized as previously described [25].

For the preparation of metal complexes, firstly, a hot methanolic solution of chalcone compound (0.01 mol & 20 ml) was prepared. Then a hot methanolic solution (0.01

mol & 20 ml) of the hydrated metal salts was added. The resulting solutions were refluxed under stirring for 4 hrs. The solid products thus separated out on hot, filtered off, washed several times with methanol and finally dried in a vacuum desiccator over anhydrous calcium(II) chloride.

2.2. Physical measurements

Perkin-Elmer 2400 CHN Elemental analyzer were performed for the elemental microanalysis of the prepared compounds in the microanalytical center, Cairo University. The Perkin-Elmer 1430 IR spectrophotometer was used for recording the Infrared spectra (as KBr discs) within the range 4000-200 cm^{-1}. TheNujol mull electronic spectra have been measured using a Shimadzu UV-Vis 240 spectrophotometer.The magnetic susceptibility of the solid chelates was carried out at room temperature by the Gouy's technique for magnetic susceptibility instrument.The Schimadzu TG-50 thermogravimetric analyzer was used for the thermogravimetric analysis (TGA) of the solid chelates with heating rate 10°C /min under nitrogen atmosphere, in the range 25-800°C.

2.3. Quantum chemical computations

The DFT computations with periodic boundary environments were accomplished applying the well-known $DMol^3$ module [28], by means of Materials Studio set [29]. The tasks were utilized as a part of combination together with the specific dual mathematical and polarization principle set DNP that is precise as Gaussian basis sets [30-32]. The RPBE (GGA) functions [33] is up to now the greatest exchange-correlation function [34] is applied to consider the exchange properties of the electrons.

2.4. Antimicrobial activity

For screening the antimicrobial activity for the tested chelates disc diffusion method was employed [35].

Freshly prepared spore suspension of different test microorganisms (0.5ml of about 10^6 cells/ml) was mixed with 9.5ml of melting sterile Sabouraud's dextrose medium (for fungi) or nutrient agar medium (for bacteria) at 45°C, poured on sterile Petri dishes, and left to solidify at room temperature. Regular cellulose filter paper discs of 6 mm diameter were prepared under aseptic conditions. Each disc was saturated with 20 mg of each tested suspended material. For each test three replicas were made. All plates were incubated at 27°C for 48 hours for fungi, and at 32°C for 24 hrs for bacteria. The average diameters of inhibition zones were recorded in millimeters. All experiments were carried out in triplicate and the mean results are evaluated.

2.5. MIC determination

Half-fold serial dilutions were made for selected chelates in order to prepare concentrations of 6.25, 12.5, 25, 50 and 100 mg/ml in distilled water, zero concentration was considered as a negative control. A previously prepared pure spore suspension of each test microorganism (0.5ml of about 10^6 cells/ml) was mixed with 9.5 ml of each concentration in sterile test tubes, incubated at 27°C for 3 days for fungi, and at 32°C for 24 hours for bacteria, then optical density of growth was measured by spectrophotometer (Optima SP-300, Japan) at 620 nm for each incubated mixture, results were represented graphically, and MIC was recorded for each tested material [36].

2.6. Measurement of Potential cytotoxicity

The human cancer cell line used for in vitro screening experiment is breast cancer cell line (MCF7). It was obtained frozen in liquid nitrogen (-180^{o}C) from the American Type Culture Collection. The tumor cell lines were maintained in the National Cancer Institute, Cairo, Egypt, by serial sub-culturing. Potential cytotoxicity of the compounds was tested using Skehan method [37]. Cells were plated in 96-multiwell plate (104 cells/well) for 24 hrs before treatment with the compound to allow attachment of cell to the wall of the plate. Different concentration of the compounds under test (0, 5, l0, 12, 25 and 50 µg/ml) were added to the cell monolayer triplicate wells were prepared for each individual dose. Monolayer cells were incubated with the compounds for 48 h at 37 °C and in atmosphere of 5% CO_2. After 48 h, Cells were fixed, washed and stained with Sulfo-Rhodamine-B stain. Excess stain was washed with acetic acid and attached stain was recovered with Tris EDTA buffer. Color intensity was measured in an ELISA reader. The relation between surviving fraction and drug cone is plotted to get the survival curve of each tumor cell line after the specified compound. An Elisa reader (TECAN

SUNRISE), Potential cytotoxicity of the compounds was measured in (Pharmacology Unit, Cancer Biology Department, National Cancer Institute, Cairo University). Doxorubicin was used as standard cytotoxins.

3. Results and discussion

3.1. Characterization of the investigated chalcone and its metal chelates

The stoichiometry and formulation of the investigated chalcone, namely; (E)-3-(4-(dimethylamino)phenyl)-1-(pyridin-2-yl)prop-2-en-1-one and its metal chelates, $[CrL_2(OAc)_2].2H_2O.AcO$, **C1**, $[MnL_2(OAc)_2].2H_2O$, **C2**, $[CuL_2].2NO_3.H_2O$, **C3**, $[ZnL_2(OAc)_2].H_2O$, **C4**, $[ZnL_2Cl_2]$. H_2O, **C5**, and $[CdL_2(OAc)_2]$, **C6** are based on their elemental, molar conductivity and IR spectral data. The results of elemental analysis and molar conductance are collected in Table 1. The isolated solid chelates are stable in air and soluble in DMF and DMSO. The low molar conductance values of all chelates except C3-Chelate (C3) revealed that these chelates are non-electrolytes in DMF [38]. The presence of Cl^- ions outside the coordination sphere was confirmed by the chemical reaction with $AgNO_3$ where the white precipitate of AgCl was observed. The addition of $FeCl_3$ solution to the acetato chelates solution gave the red brown coloration, confirming the presence the of acetate ions outside the coordination sphere. Our efforts to obtain crystalline samples of the compounds of X-ray crystal structure were unsuccessful, we decided to carry out molecular modeling studies in order to gain a better understanding of the structures of the metal complexes.

3.2. IR spectra

In order to study the binding mode of chalcone to the metal ions, the IR spectrum of the free chalcone was compared with the spectra of the corresponding metal chelates. The important infrared bands exhibited by the organic chalcone and its chelates are given in Table 2. A cursory glance on the data reported in Table 1, it was found that the strong and intense chalcone band at $1648 cm^{-1}$ which was due to $\upsilon_{C=O,}$ showed shift to lower frequencies ($40\text{-}62\ cm^{-1}$) in the case of chelates. This shift is due to coordination of carbonyl oxygen to the metal center. The coordination of oxygen atom to the metal center has been supported by the appearance of non-chalcone bands within the range 520-596 cm^{-1}, due to $\upsilon_{M\text{-}O}$. The $\upsilon_{C=N}$ of the pyridine ring of the free chalcone appeared at 1519 cm^{-1}, was shifted to higher value on chelate formation, due to the coordination of nitrogen atom to the central metal ion. This observation was confirmed by the appearance of a new band ($\upsilon_{M\text{-}N}$) at 403- 447cm^{-1}.The presence of lattice or coordinated water molecules in metal chelates has been indicated by the band appearing within the range 3424-3338cm^{-1}, corresponding to υ_{OH} of water molecules. The IR spectrum of C3-chelate exhibits three bands at 1460 (υ5), 1375 (υ1) and 1222 (υ2) cm^{-1} corresponding to monodentate coordination of nitro group [39]. New two bands appearing in the spectra of chelates (C1-C4) located within the ranges 1444-1477and 1315-1330cm^{-1} are assigned to υ_{COO} (asy) and υ_{COO}(sym), respectively. The difference between these two bands (Δυ)indicated the coordination nature of the acetate as a mondentate chalcone [40].

3.3. Electronic spectra and magnetic moments

The magnetic moment C1-chelate (μ_{eff}=3.77 BM) corresponded to the spin only value for three unpaired electrons due to the absence of any orbital contribution [41]. The electronic spectrum of C1-chelate shows bands at bands at 17391and 25317 cm^{-1}assignable to $^4A_2g \rightarrow {}^4T_2g$ (F) v_1 and$^4A_2g \rightarrow {}^4T_1g$ (F) v_2,respectively,in an octahedral geometry [42].The three spin allowed transitions of Cr(III) in an octahedral field are as follows:

$$^4A_2g\ (F) \rightarrow {}^4T_2g(F)(v_1),\ \ {}^4A_2g\ (F) \rightarrow {}^4T_1g(F)(v_2), {}^4A_2g\ (F) \rightarrow {}^4T_1g(P)(v_3).$$

The $v_1$transitions is a direct measurement of the chalcone field parameter 10Dq.From v_1 and v_2, the value of B and β can be calculated.The B value is calculated by [43]

$$B =[2v_1^2 -3\, v_1\, v_2+ v_2^2][15\, v_1-27\, v_1]$$

and the value of β is computed is $B=(B \mid B^O)$ where B^O =918 cm^{-1}.

The calculated values of Dq (1786),B , β and $v_2 \,/\, v_1$ values as well as the magnetic moments confirm an octahedral environment.

$$B = 835.4 \qquad \beta=0.91 \qquad v_2 / v_1=1.456 \qquad v_1=10Dq$$

The Nujol mull spectrum of C2-chelate exhibited four absorption bands at 17857, 24390, 28571,and 29412 cm^{-1}. These bands may assigned to the transition: $^6A_{1g} \rightarrow {}^4T_{1g}$ (^{4}G), $^6A_{1g} \rightarrow {}^4Eg, {}^4A_{1g} \rightarrow$ (^{4}G) (10B+5C),$^6A_{1g} \rightarrow {}^4Eg$ (^{4}D) (17B+5C) and$^6A_{1g}$ → $^4T_{1g}$ (^{4}p) (7B+7C),respectively, corresponding to the octahedral geometry.The second and third transitions are free from the crystal field splitting [44]. Thus, the parameters B and C were calculated from these transitions. The calculated Dq, B, C and B are 1786, 597, 3684 cm^{-1} and 0.76, respectively. The value of β indicated the appreciable covalent character of metal chalcone σ-bond. The magnetic properties calculated for C2-chelate show strikingly subnormal values (2.43 BM) has been ascribed to anti-ferromagnetism.

The effective magnetic moment value of C3-chelate (1.92 BM) indicated that Cu(II) chelate is monomeric in nature and the absence of Cu-Cu interaction. C3-chelate shows an intense broad band at 16667 cm^{-1}which may be assigned to$^2B_{1g}$ → ^2E_g. This suggest the distorted octahedral geometry for C3-chelate. The broadness of this band may be due to Jahn-Teller distortion of the octahedral geometry [45]. The band observed at 28735 cm^{-1} refers to chalcone-metal charge transfer transition.

3.4. Thermal analysis

The thermal behavior of metal chelates was studied by means of TGA techniques. The data including the stages of decomposition, temperature ranges, peak temperatures, decomposition product loss, found and the calculated mass loss percentages are listed in Table 3. The obtained data indicated that all the metal chelates underwent thermal decomposition within two, three or four stage decomposition processes.

C1-chelate decomposed in four successive decomposition steps. The first step appeared within the temperature range 28-65^{o}C which assigned to the loss of lattice water. The second step appeared within the range 113-218^{o}C was assigned to the elimination of lattice OAc anion. The third step of decomposition appeared within the ranges 218-311^{o}C, corresponded to the elimination of coordinated OAc anion. The last step of decomposition (311-442^{0}C) corresponded to further decomposition of the organic chalcone. The final product of decomposition left behind assigned as the thermally stable Cr_2O_3 +C.

The metal chelates C2-C5 gave three-stage decomposition processes. The first step of decomposition appeared within the temperature ranges19-118, 24-75, 24-80 and 25-80^{o}C, respectively and assigned to the loss of lattice water. The second step appeared within the temperature ranges 128-274, 171-226, 116-243, and 161-234^{o}C for chelates C2, C3, C4 and C5, respectively, corresponding to the loss of coordinated anions. The third step of decomposition appeared at temperature ranges 282-491, 226-

384, 243-536 and 234-656^{o}C for chelates C2,C3, C4, C5, respectively, due to the decomposition of organic chalcone and resulting in the formation of MnO, CuO + 2Cu, Zn and ZnO, as final product for chelates C2,C3, C4 and C5, respectively.

The metal chelate C6 gave two-step decomposition diagram. The first one of decomposition within the temperature ranges 87-258^{o}C corresponded to the loss of coordinated acetate anion. The last one of decomposition within the temperature at 258-630^o Ccorresponded to the further decomposition of the organic chalcone with the formation of CdO as a final product.

The kinetic parameters of activation energy (E), reaction order (n) and Arrhenius pre-exponential factor (A) as well as the thermodynamic parameters were calculated from the integral method proposed by Coats-Redfern [46], Figure S1

The thermodynamic parameters of activation (ΔH*, ΔS* and ΔG*) were estimated according to the previous methods with the aid of the following expressions:

$\Delta H^* = E - RT$, $\Delta S^* = R \ln (hA / K_B T)$, $\Delta G^* = \Delta H^* - T\Delta S^*$

where ΔH* is the activation enthalpy (kjmol^{-1}), ΔS* is the activation entropy (Jmol^{-1}k^{-1}), ΔG* is the Gibbs activation free energy (kjmol^{-1}), h is the Plank constant, K_B is the Boltzmann constant and T is the observed peak temperature.

From the results listed in Table 4, one can pointed out the following remarks:

i. The thermodynamic parameters (ΔH*, ΔG*, and ΔS*) of the decomposition steps are affected by the nature of the metal ion in the formed chelate.
ii. The positive sign of ΔH* indicates that the decomposition stages are endothermic processes.
iii. The high values of E revealed high stability of the chelates due to their covalent bond character.
iv. The positive sign of ΔG* for most investigated chelates revealed that all the decomposition steps are non-spontaneous processes. Also, the values of ΔG* increases significantly for the subsequent decomposition stages of a given chelate. This is due to increasing the values of TΔS from one step to another which overrides the values of ΔH*.
v. The negative values of entropy of activation indicated that the activated chelates have a more ordered structure than the reactants.

3.5. Molecular orbital calculations

3.5.1. IR analysis

Theoretical and experimental IR spectra Figure S2 were scaled to produce the spectroscopic signs of chalcone which displays that υC=O band (measured: 1648 cm$^-$

^{1}, predicted: 1660 cm^{-1}) and υC=N band (measured: 1519 cm^{-1}, predicted: 1578 cm^{-1}). The small differences among the measured frequencies is due to the predicted spectrum was performed in vacuum, while the measurements were refined for solid state. The lower symmetry is the main reason for the chelateity of the vibrational modes of the investigated chalcone. Especially, torsion, all plane modes are difficult to allocate due to decipher by the ring modes besides the imitative. Nevertheless, the existence of some obvious vibrations supportive to depict in the obtained figure.

3.5.2. Geometry optimization

For the optimized structural models, Figures S3-S9, inspection of the bond distances and angles Tables 5 and 6, the following remarks could be outlined:

1. The active groups (C=O and C=N$_{py}$) are elongated upon coordination with metal ion. This is referred to the formation of M-N and M-O bonds [27], which let the C=N and C=O bonds become weaker.
2. The M-N and M-O bond distances are in a good agreement with the sum of covalent radii for M and N or O atoms and similar to values repeated earlier [47].
3. In all chelates, the bond distances of M-Cl and/ or M-OAc are longer than M-N and M-O.
4. The length of Zn-Cl bond in chelate C5 are longer than that of Zn-OAc bond in C4 chelate.
5. The bond angles of C1, C2, C4, C5 and C6 are similar to that reported for an octahedral chelate with d^{2}sp^{3} or sp^{3}d^{2} hybrid orbitals and a square planar geomtery with sp^{2}d hybrid orbitals [48] for C3 chelate.

3.5.3. Chemical reactivity

3.5.3.1. Global reactivity descriptors

Highest Occupied Molecular Orbitals "HOMO level" is defined as is the one which essentially shows an electron donation behavior. While, the Lowest Unoccupied Molecular Orbital "LUMO" is one which significantly acts as an electron acceptor. Both named frontier molecular orbitals (FMOs) (Figures 1-7, supplementary materials) estimate the electric optical properties, electronic transitions and kinetic stability [49]. The FMOs hypothesis anticipate sites of coordination (electrophilic attack) on an aromatic compound. The interaction between HOMO of one moiety with LUMO on another one is a major reason in most of the reactions. We can demonstrate from the computation that the oxygen of the C=O group have the largest values of molecular orbital coefficients showing that it is a suitable site of chelation.

The energy gap ($\Delta E= E_{HOMO}$ - E_{LUMO}), chemical descriptors as softness (S), hardness (η), electronegativity (χ), chemical potential (μ) and (electrophilicity) (ω), softness (σ) and additional electronic charge (ΔN_{max}) for the isolated compounds was done as illustrated in Table 7**.** These descriptors can be estimated using the equations described previously [50], as well as the inverse value of the global hardness, (which is designed as the softness, σ , σ =1/ η) and the maximum number of electrons transferred in a chemical reaction (ΔNmax=- μ /η), have been calculated as mentioned previously [51]:

According to the obtained results as summarized in Table 8, it was exhibited that:

i. The E_{HOMO} and E_{LUMO} are almost negative showing the stability of the isolated compounds [52, 53].

ii. Gutmann’s variation rules, "the bond strength increases as the neighboring bonds become weaker" such as found by Linert et al. [54]. This interpretation agrees well with the resultant as the increase of the E_{HOMO} is convoyed by a weakness (elongation) of the metal–chalcone bond, which prompts a reinforcing (shortness) of the sites next to the metal chalcone centers.

iii. A hard molecule is represented by large HOMO-LUMO difference, while a soft and more active framework has a small energy difference. Chemical potential 'μ' that estimates the escaping capability of electrons from its equilibrium framework diminishes as follow C2 (-3.027) > C1 (-3.076) > chalcone (-3.608) > C3 (-3.647) > C4 (-3.758)> C5 (-3.804)> C6 (-3.811).

iv. The importance of η and σ is to measure the molecular stability and reactivity. In a chelate formation system, metal ions are Lewis acid (soft acids) and thus Lewis base (soft base) chalcones are most effective for chelate formation. Accordingly, it is concluded that the investigated chalcone with a proper σ value has a good tendency to chelate metal ions effectively [55].

v. ΔN_{max} is a reactivity index that measures the stabilization in the energy of the compound. The calculation of ΔN_{max} displayed that C1 and C2 have the higher values (14.578 e and 12.480 e), respectively than chalcone and other chelates which confirm that both chelates C1 and C2 have the higher facility to accept electrons (electrophiles).

The calculations of the total energy, Table 8**,** revealed that the increase of the value of the calculated binding energy of chelates compared to that of the chalcone indicates that the stability of the formed metal chelates is higher than that of chalcone. The dipole moment values of the chelates are larger than the chalcone value except the dipole moment of chelates (C3) and (C4) has a lower value than that of chalcone. The structure activity relationship studies were investigated to correlate the antimicrobial properties of the studied compounds that related to physico-chemical properties. The dipole moments are the property of interest which gives some insight on the degree of hydrophobicity/hydrophilicity of the compounds. As dipole moment decreases the polarity decreases. Thus, the lipophilic nature of the compound increases, which favors its permeation through the lipid layer of the microorganism, then destroying them.

3.5.3.2. Local reactivity descriptors

The most relevant local descriptor of reactivity is the Fukui function (FF). The Fukui function shows the propensity of the electronic density to deform at a given position upon accepting or denoting electrons [56-58] which are more prone to undergo a nucleophilic or an electrophilic attack, respectively. The Fukui function is defined as [56];

$$f(\mathrm{r}) = \frac{\delta\rho(r)}{\delta N} r$$

where ρ(r) is the electronic density, N is the number of electrons and r is the external potential exerted by the nucleus. The local (condensed) Fukui functions (f_k^+, f_k^-, f_k^o) are calculated using the following equations:

$f_k^+ = [q_k(n+1) - q_k(N)]$ for nucleophilic attack

$f_k^- = [q_k(N) - q_k(N-1)]$ for electrophilic attack

$f_k^o = 1/2\,[q_k(N+1) + q_k(N-1)]$ for radical attack

Where q_k is the atomic charge (evaluated from Mulliken population analysis, electrostatic derived charge, etc.) at the kth atomic site is the neutral (N), anionic (N+1) or cationic (N-1) chemical species.

Also local softness(S_k^+, S_k^-, S_k^o) and electrophilicity indices (ω_k^+, ω_k^-, ω_k^o) are calculated [59] using the following equations:

$S_k^+ = S f_k^+$, $S_k^- = S f_k^-$, $S_k^o = S f_k^o$

$\omega_k^+ = \omega f_k^+$, $\omega_k^- = \omega f_k^-$, $\omega_k^o = \omega f_k^o$

Where +, -, 0 signs show nucleophilic, electrophilic and radical attack respectively.

The reactivity indexes (f_k^+, f_k^-, f_k^o) are directly disturbed with the selectivity of the molecule to specific chemical events. The Fukui functions are calculated for chalcone and its chelates as shown in Tables (S1-S7, supplementary materials). The ordering of the nucleophilic, electrophilic and radical attack sites for chalcone chalcone and its chelates is shown in Table 9. It is clear that the substitutions of OAc group and Cl atom in the chelates leads to a redistribution of electron density.

From the values reported in Table S1, supplementary materials, the reactivity order for the nucleophilic case as O(14)>N(18)>C(16). The calculated f_k^- value predicts that the possible sites for electrophilic attack is O(14)>C(2)>C(13) site and the radical attack was predicted as O(14)>N(18)>C(20) site. İt has been found that the results for chalcone predict the highest f_k^+, f_k^- and f_k^o value for O(14) indicates the most favored site for all attacks. Thus, a profound dual descriptor *Δf(r)* which is the difference between the nucleophilic and electrophilic Fukui functions is explained by the following equation [60]:

$$\Delta f(r) = f_k^+ - f_k^-$$

If *Δf(r)*>0, then the site is favored for a nucleophilic attack, whereas If *Δf(r)*<0, then the site is favored for an electrophilic attack. So, the calculation of *Δf(r)* for O(14) is smaller than zero indicate that O(14) is most favored site for electrophilic attack. The reflection of the reactive sites by S_k^+ for chalcone and its chelates are found almost identical to f_k^+. Even though the values are numerically less, the ordering of the reactivity for S_k^+ has not changed.

3.5.4. Molecular electrostatic potential (MEP)

It is considered as a graph of electrostatic potential charted onto the constant electron density surface. It is additionally remarkably valuable in research of sub-atomic structure with its physiochemical property association and hydrogen bonding interactions [61-63]. The electrostatic potential V*(r)* at a given point r (x, y, z) is characterized as a function of the interaction energy between the electrical charge produced from the electrons, nuclei and protons **placed at r** [64]. Calculation of electrostatic potential is feasible for atoms utilizing the Γ-point and various k-points. In the current investigation, 3D plots of molecular electrostatic potential (MEP) of chalcone and its metal chelates (Figures 8-14) have been figured. The largest negative part, which desired site for electrophilic attack indications as red covering, the largest positive area that desired site for nucleophilic attack designated by the blue color. The potential decreases as follow: red < green < blue, where blue demonstrates the most favored site for the attraction while the red one reveals the greatest site for the repulsion. Areas having the negative potential are over the electronegative molecules while the regions having the positive potential are over the hydrogen atoms.

3.5.5. *Mulliken atomic charges*

Mulliken atomic charge estimation of chalcone and its chelates, Figure 15 and Tables S8-S14 in the supplementary materials shows a significant role in the procedure of theoretical estimation of the molecular framework. Figure 15 explains the charge distribution of chalcone. Oxygen and nitrogen atoms having negative values due to their giving capacity. In contrast, hydrogen atoms and most of carbon atoms displayed positive values because of its accepting capacity. According to the above results, the structures of the chelates were shown in Scheme 1.

3.6. *Biological screening*

The investigated metal chelates, C1-C6 were evaluated for their antimicrobial activity in comparison with the organic chalcone using agar diffusion technique [35]. The tested organisms are Gram-negative bacteria (*E. coli*),Gram-positive bacteria (*S. aureus*) and Fungi (*C. albicans*&*A. niger*). The screening results are summarized in the Table 10 and represented in Figure S10. Generally, the investigated chelates have lower activity than the chalcone.

In the present case, the activity is dependent on the central metal ion and its ability to diffuse into the cell membrane of the organism. The antimicrobial activity of the chelates can be ordered as C5> C1 > C2, suggesting that the lipophilic behavior increases in the same order. Zn(II) chelate had a higher activity against the bacteria and fungi strains. C5 and C2 chelates showed better antimicrobial activity against Gram negative bacteria. Chalcone and its C1 chelate showed a highest activity towards positive bacteria.

The variation in the activity of different chelates against different microorganisms depends either on the impermeability of the cells of the microbes or differences in ribosomes in microbial cells **[65].** The data listed in Table 10 indicated that all the tested compounds showed a moderate to good antimicrobial activity against the tested microorganisms when compared with the standard drugs, except for *A. niger*.

The tested chalcone and its C1 chelate were more active against Gram-positive than Gram-negative bacteria, while C2 and C5 chelates have more activity against negative than positive bacteria. It may be concluded that the antimicrobial activity of the compounds is related to cell wall structure of the bacteria. It is possible because the cell wall is essential to the survival of bacteria and some antibiotics are able to kill bacteria by inhibiting a step in the synthesis of peptidogly can. Gram-positive bacteria possess a thick cell wall containing many layers of peptidogly can and teichoic acids, but in contrast, Gram negative bacteria have a relatively thin cell wall consisting of a few layers of peptidogly can surrounded by a second lipid membrane containing lipopolysaccharides and lipoproteins. These differences in cell wall structure can produce differences in antibacterial susceptibility and some antibiotics can kill only Gram-positive bacteria and is infective against Gram-negative pathogens [66]. Furthermore, the minimum inhibitory concentrations (MIC) of chalcone against microorganisms are show in Table 11.

3.7. Antitumor measurements

The cytotoxic effect of the different concentration of the chalcone and its metal chelates in the concentration rang of 0, 5, 12.5, 25 and 50 µg/mg was tested against human breast cancer cell line (MCF7). The IC_{50} (half maximal inhibitory concentration value) which measures the effectiveness of a compound to inhibit biological or biochemical functions, is derived from the experimental data. For comparison,the cytotoxicity of the standard doxorubicin antitumor drug was evaluated under the same conditions

The results obtained are presented in Figure S11. This figure shows that the proliferation of MCF_7 is decreased upon increasing the concentration of the chalcone and its chelates. i.e the toxicity of these compounds was found to be concentration dependent. The data indicate that the *in vitro* IC_{50} values for the metal chelates are higher than the free chalcone, therefore the free chalcone possess better antitumor activity than the metal chelates. This means the chelates failed to cause significant inhibitory action on the tumor cell as is evident from its high cell IC_{50}value.

From the data obtained, it is possible to exhibit the relation between IC_{50}value and the nature of the metal ion. However, the toxicity of the metal complexes can be related to the strength of metal-ligand bonds in addition to other factors such as the size of the metai ion . The higher the size of the metal ion, the higher the value of IC_{50}. [69]

Cr(III) complex exhibited more potential anticancer activity than the other metal complexes. Thus, Cr(III) chelate is more effective than the other chelates towards cancer cell line.

[69]R.R.Zaky[a]T.A.Yousef[b] K.M.Ibrahim[a] Co(II), Cd(II), Hg(II) and U(VI)O_2 complexes of *o*-hydroxyacetophenone[*N*-(3-hydroxy-2-naphthoyl)] hydrazone: Physicochemical study, thermal studies and antimicrobial activity, Spectrochimica Acta Part A: 97 (2012) 683-694

According to Shier [70] compounds with IC_{50} within the range of 10-25 µg/ml are considered weak anticancer drugs, while those of IC_{50} between 5 and 10 µg/ml are moderate and compounds of activity below 5.00 µg/ml are considered strong agents. Based on these facts, it is clear that the C1 chelate has a moderate anticancer activity, the chalcone exhibited strong activity while the other chelates exhibited a weak antitumor activity according to Shier scale. Also, the results showed that the chelates under investigation give higher IC_{50} values [71-74] or lower **[75]** for breast cell MCF7 than the reported for cytotoxic metal (II) chelates for the same cell .

The crucial aim of structure activity relationship(SAR)[76] is to correlate the biological properties with different quantum chemical descriptors such as the energy gap ($\Delta E= E_{HOMO} - E_{LUMO}$), hardness (η), electronegativity (χ), chemical potential (µ) and (electrophilicity) (ω), softness (σ) and additional electronic charge (ΔN_{max}). These values showed no clear direct correlation with the anticancer activity.

A property of interest is the dipole moment. The highest dipole moment value of the Cr(III) complex should be a considerable factor fot its highest cytotoxicity[77] compared to the other complexes. The results were correlated with the experimental data. The antibacterial activity of the chalcone and its chelates have been tested. The data indicated that all the metal chelates demonstrated a higher activity than the free chalcone. The results suggested that:(i)Cr(III) complex has an enormous potential as anticancer agent compared to the other chelates, (ii) All the metal chelates a lower activity compared to the free chalcone [78]

4. Conclusion

Cr(III), Mn(II), Cu(II) Zn(II) and Cd(II) chelates of the titled chalcone have been synthesized and characterized by analytical and spectral methods. The data indicated that the investigated chalcone acts as a bidentate chalcone coordinated to the metal ions via the O and N atoms of the C=O and C=N groups, respectively. The spectral and magnetic data revealed the formation of octahedral chelates for all chelates except Cu(II) chelate which exhibit the square planar geometry. The thermal properties of the metal chelates have been investigated by TGA technique. The kinetic and thermodynamic parameters of the decomposition steps have been calculated. Molecular orbital calculations have been performed for the chalcone and its chelates. The antibacterial activity of the chalcone and its chelates have been tested. The data indicated that all the metal chelates demonstrated a higher activity than the free chalcone. The results suggested that:(i)Cr(III) complex has an enormous potential as anticancer agent compared to the other chelates, (ii) All the metal chelates a lower activity compared to the free chalcone . All chelates exhibited a very weak antitumor activity except Cr (III) chelate which has a relatively stronger antitumor activity, while the antitumor activity of these chelates is not as strong as that of chalcone.

Based on the data of the manuscript, the structure of chalcone chelates are represent as:

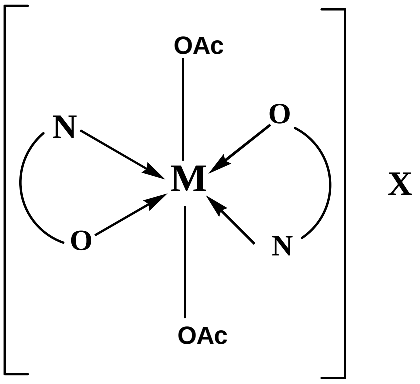

X = $2H_2O$, AcO for C1; $2H_2O$ for C2; H_2O for C4; Zero for C6

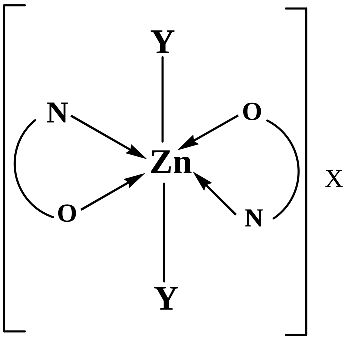

Y = Zero, X= $2NO_3 .H_2O$ for C3; Y = Cl, X= H_2O for C5

Scheme 1: The structure of chalcone compoundand its chelates.

References

[1] D. Kumar, N. M. Kumar, K. Akamatsu, E. Kusaka, H. Harada, T. Ito, Synthesis and biological evaluation of indolyl chalcones as antitumor agents. Bioorg. Med. Chem. Lett. 20 (2010) 3916 - 3919.

[2] Z. Ratkovic, Z. Juranic, T. Stanojkovic, D. Manojlovic, R. Vukicevic, N. Radulovic, M. Joksovic. Synthesis, characterization, electrochemical studies and antitumor activity of some new chalcone analogues containing ferrocenylpyrazole moiety. Bioorg. Chem. 38 (2010) 26-32.

[3] J. Biradar, B. Sasidhar, R. Parveen,Synthesis, antioxidant and DNA cleavage activities of novel indole derivatives. Eur. J. Med. Chem. 45 (2010) 4074–4078.

[4] L. Tavares, S. Johann, T. Alves, J. Guerra, et.al., Quinolinyl and quinolinyl N-oxide chalcones: synthesis, antifungal and cytotoxic activities. Eur. J. Med. Chem. 46(2011) 4448-4456.

[5] A.M. Asiri, S.A. Khan. Synthesis and Anti-Bacterial Activities of a Bis-Chalcone Derived from Thiophene and Its Bis-Cyclized Products. Molecules. 16 (2011) 523–531.

[6] F. Smit, D. N’Da. Synthesis, in vitro antimalarial activity and cytotoxicity of novel 4-aminoquinolinyl-chalcone amides. Bioorg. Med. Chem. 22 (2014)1128–1138.

[7] F. Smit, R. van Biljon, L. Birkholtz, D. N'Da. Synthesis and in vitro biological evaluation of dihydroartemisinyl-chalcone esters. Eur. J Med Chem. 90 (2015) 33–44.

[8] F. J. Smit, J. J. Bezuidenhout, C. C. Bezuidenhout, D. D. N'Da. Synthesis and in vitro biological activitie of ferrocenyl-chalcone amides. Med Chem Res. 25 (2016) 568–584.

[9] J. Maynadie, B. Delavaux-Nicot, D. Lavabre, S. Fery-Forgues. Monosubstituted ferrocenyl chalcones: Effect of structural changes upon the ability to detect calcium by absorption spectroscopy. J. Organomet. Chem. 691 (2006) 1101-1109.

[10] B. Delavaux-Nicot, J. Maynadie, D. Lavabre, S. Fery-Forgues. Ferrocenyl Compound as a Multiresponsive Calcium Chemosensor with Remarkable Fluorescence Properties in CH_3CN. Inorg. Chem. 45 (2006) 5691-5702; B.Delavaux-Nicot, J. Maynadie, D. Lavabre, S. Fery-Forgues, Two electroactive ferrocenyl chalcones as original chemosensors for $Ca^{2\%20}$ and $Ba^{2\%20}$ cations in CH_3CN. J. Organomet. Chem. 692 (2007) 3351-3362.

[11] S. Lee, Y. Noh, K. Son, D. Noh. Chromotropic Ferrocenyl Chalcone with two Pyrenyl Groups: Solvatochromism and Molecular Chemosensor for Fe(III)/Fe(II) ions. Inorg. Chem. Commun. 13 (2010) 1343-1346.

[12] B. Meric, K. Kerman, D. Ozkan, P. Kara, A. Erdem, O. Kucukoglu, E. Erciyas, M. Ozsoz. Electrochemical biosensor for the interaction of DNA with the alkylating agent 4,4'-dihydroxy chalcone based on guanine and adenine signals. J. Pharm. Biomed. Anal. 30 (2002) 1339-1346.

[13] M. Muthukumar, P. Viswanathamurthi. Spectral, catalytic, and antifungal studies of ruthenium(II) chalcone chelates. J. Coord. Chem. 63 (2010)1263- 1272

[14] P. Rishikesh, S. Dubey, R. Gaur, R. Koiri, B. Maurya, S. Trigun, L. Mishra. Structural characterization and cytotoxicity studies of ruthenium(II)–dmso–chloro chelates of chalcone and flavone derivatives. Polyhedron. 29 (2010) 1055-1061; S. Attar, Z.Brien, H. Alhaddad, M. Golden, A. Calderon-Urrea. Ferrocenyl chalcones versus organic chalcones: a comparative study of their nematocidal activity. Bioorg. Med. Chem. 19 (2011) 2055-2073.

[15] M. Kalanithi, M. Rajarajan, P. Tharmaraj, C. Sheela. Spectral, biological screening of metal chelates of chalcone based Schiff bases of N-(3-aminopropyl) imidazole. Spectrochim. Acta A. 87 (2012) 155-162.

[16] J. Da Silva, A. Despaigne, S. Louro, C. Banderia, E. Souza-Fagundes, H. Beraldo. Cytotoxic activity, albumin and DNA binding of new copper(II) chelates with chalcone-derived thiosemicarbazones. Eur. J. Med. Chem. 65 (2013) 415-426; B. Thaker, R. Barvalia. Bidentate coordinating behaviour of chalcone based chalcones towards oxocations: VO(IV) and Mo(V). SpectrochimActa A. 112 (2013) 101-109.

[17] M.M. El-Sayed Aly, H.H. Fodah, S.Y. Saleh. Antiobesity, antioxidant and cytotoxicity activities of newly synthesized chalcone derivatives and their metal chelates. Eur. J. Med. Chem. 76 (2014) 517-530; E.R. Agharia. Infrared Spectroscopic Investigations of Effect of Strong Resonance Stabilized Intramolecular Hydrogen Bonding in 1-(1-Hydroxy-2-naphthyl)-3-(phenyl or Substituted phenyl)-prop-2-en-1-ones and on their Chelateation with Some Transition Metals .Chem. Sci. Tran. 4 (2015) 463-477.

[18] R. Krikavova, J. Vanco, Z. Travnicek, J. Hutyra, Z. Dvorak. Design and characterization of highly in vitro antitumor active ternary copper (II) chelates containing 2′-hydroxychalcone chalcones. J. Inorg. Biochem. 163 (2016) 8-17.

[19] A. K. Singh, G. Saxena, S. Dixit, Hamidullah, S. K. Singh,M. Arshad, R. Konwar. Synthesis, characterization and biological activities of some Ru(II) chelates with substituted chalcones and their applications as chemotherapeutics against breast cancer. J.Mol.Struct.111(2016) 90-99; H. Karaca, B. Çayegil and S. Sezer. Synthesis characterization and metal sensing applications of novel chalcone substituted phthalocyanines. Synthetic Metals. 215 (2016)134-141.

[20] M. Kalanithi, M. Rajarajan, P.Tharmaraj and C. D. Sheela. Spectral, biological screening of metal chelates of chalcone based Schiff bases of N-(3-aminopropyl) imidazole. SpectrochimActa A. 78(2012) 155-162.

[21] S.T.A.Djedouani, D. Aggoun, I. Warad, S. Rahmouni and H. Fouzi. New Cu (II), Co(II) and Ni(II) chelates of chalcone derivatives: Synthesis, X-ray crystal structure, electrochemical properties and DFT computational studies. J.Mol.Struc. 1155(2018) 11-20.

[22] A. Tajammal, M. Batool, A. Ramzan, M. M. Samra, I. Mahnoor, F.Verpoort, I. Irfan, A. G. Al-Sehemi, M. A. Munawar and M.A.R. Basra. Synthesis, antihyperglycemic activity and computational studies of antioxidant chalcones and flavanones derived from 2,5 dihydroxyacetophenone. J.Mol.Struct. 1148(2017) 512-520; M. Muthukumar and P.Viswanathamurthi. Ruthenium(II) chalconate chelates: Synthesis, characterization, catalytic, and biological studies. Spectrochim. Acta A.74(2009) 454-462; M. Muthukumar,P. Viswanathamurthi, K. Natarajan. Synthesis and spectral characterization of 2′-hydroxy chalconate chelates of ruthenium(II) and their catalytic and biological applications. Spectrochim. Acta A.70(2008) 1222-1226.

[23] S. El-Daly, M. Gaber, S. Al-Shihry, Y. El-Sayed, Photophysical properties, excitation energy transfer and laser activity of 3-(4′-dimethylaminophenyl)-1-(2-pyridinyl) prop-2-en-1-one (DMAPP): a new potential laser dye. J. Photochem. Photobiol. 195 (2008) 89-98.

[24] M.Gaber, S.A. El-Daly, Y.S. El-Sayed, Synthesis, spectral, thermal and theoretical studies of Cu(II) chelates with 3-[4′-dimethylaminophenyl]-1-(2-pyridyl)prop-2-en-1-one (DMAPP). J. Mol. Struct. 922 (2009) 51-57.

[25] M. Gaber, S. El-Daly , T. Fayed, Y. El-Sayed, Synthesis , spectral, thermal studies and electrical conductivity of Co (II) and Ni (II) chelates 3-[4-dimethylaminophenyl]-1-(2-pyridyl)prop-2-en-1-one (DMAPP). J. Lumin. 157(2015) 1–9.

[26] Y.S. El-Sayed, M. Gaber. Studies on chalcone derivatives: Chelate formation, thermal behavior, stability constant and antioxidant activity. Spectrochim. Acta A. 137 (2015) 423-431.

[27] M. Gaber, Tarek A. Fayed, Marwa N. El-Nahass, H. A. Diab, Mohammed M. El-Gamil. Synthesis, spectroscopic characterization and biological evaluation of a novel chemosensor with different metal ions. Appl. Organometal. Chem. 2019;e5133.

[28] X. Wu, A.K. Ray, Density-functional study of water adsorption on the PuO_2 (110) surface, Phys. Rev. B 65 (2002) 085403 (1-7).

[29] Modeling and Simulation Solutions for Chemicals and Materials Research, BIOVIA Materials Studio, Accelrys software Inc., San Diego, USA, 2017.

[30] B. Delley, D.E. Ellis, A.J. Freeman, E.J. Baerends, D. Post. Binding energy and electronic structure of small copper particles. Phys. Rev. B 27(4) (1983) 2132-2144.

[31] B. Delley, An all-electron numerical method for solving the local density functional for polyatomic molecules, J. chem. phys. 92 (1990) 508-517.

[32] B. Delley, From molecules to solids with the DMol 3 approach, J. Chem. Phys. 113(18) (2000) 7756-7764.

[33] B. Hammer, L.B. Hansen, J.K. Nørskov, Improved adsorption energetics within density-functional theory using revised Perdew-Burke-Ernzerhof functionals, Phys. Rev. B 59(11) (1999) 7413-7421.

[34] A. Matveev, M. Staufer, M. Mayer, N. Rösch, Density functional study of small molecules and transition-metal carbonyls using revised PBE functionals, Int. J. Quantum Chem 75 (1999) 863-873.

[35] R.E. Cooper, Analytical Microbiology, F.W. Kavanageh, Vol. 1 & 11, Academic press, New York & London, 1972, T. Pridham, L. Lindenfelser, O. Shotwell, F. Stodola, R. Benedict, C. Foley, P. Jacks, W. Zaumeyer, W. Perston, Antibiotics against plant diseases: A laboratory and green house survey. J. Mitchell. Phytopathology. 46 (1956)568-75.

[36] S. Shadomy, I. Epsinel, R. Cartwright,: Laboratory studies agents:Susceptibility test and bioassays. In: Lennette A, Balows W, Hausler H, and Shadomy S 4th ed. of: Manual of Clinical Microbiology, Little Brown Co., Boston, 1985.

[37] P. Skehan, R. Storeng, New Colorimetric Cytotoxicity Assay for Anticancer-Drug Screening. J. Natl Cancer Inst. 82 (1990) 1107-1112.

[38] W.J. Geary, The use of conductivity measurements in organic solvents for the characterisation of coordination compounds. Coord. Chem. Rev. 7 (1971) 81-122.

[39] K. Nakamoto, Infrared and Raman spectra of coordination compounds, Wiley Interscience, New York, 1970.

[40] K. Nakamoto, Infrared spectra of inorganic and coordination compounds. New York, Wiley and Sons, 1986.

[41] U. El-Ayaan, I.M. Kenawy, Y.G. Abu El-Reash, Synthesis, thermal and spectral studies of first-row transition metal chelates with girard P reagent-based chalcone. Spectrochim. Acta A. 68 (2007) 211-219.

[42] O. Adly, Synthesis, Molecular Modeling, Thermal and Spectral Studies of Metal Chelates of Hydrazone Derived From 5-Acetyl-4-Hydroxy-2h-1,3-Thiazine-2,6(3h)-Dione and Thiosemicarbazide. Spectrochim. Acta A. 79 (2011) 1295-1303; O. A. Gammal, R. El-Shazly, F. El-Morsy, A. El-Asmy, Synthesis, Characterization, Molecular modeling and Biological Activity of N1,N2-Bis(1-(pyridin-2-yl) ethylidene)oxalohydrazide and its Metal Chelates. J. Mol. Struct. 998 (2011) 20-29.

[43] E. R. Price,J.R.Wasson, Chelates with sulfur and selenium donors-X chromium(III) piperidyldithiocarbamates. J. Ionrg. Nucl. Chem. 36 (1974) 67-71.

[44] S. Chandra, L. Gupta, D. Jain, Spectroscopic Studies on Mn(II), Co(II), Ni(II), and Cu(II) Chelates With N-Donor Tetradentate (N4) Macrocyclic Chalcone Derived From Ethylcinnamate Moiety. Spectrochim.Acta A. 60 (2004) 2411-2417.

[45] A.A. Emara, O.M. Adely, Synthesis and spectroscopic studies of new binuclear transition metal chelates of schiff bases derived from 4,6-diacetylresorcinol. Transition Met. Chem. 32 (2007) 889-901.

[46] A.W. Coats, J.P. Redfern, Kinetic Parameters from Thermogravimetric Data. Nature. 201 (1964) 68-69; I. McDonald, J. Thornton. Satisfying hydrogen bonding potential in proteins. J. Mol. Biol. 238 (1994) 777–793.

[47] K. Fukui, T. Yonezawa, C. Nagata, H. Shingu, Molecular orbital theory of orientation in aromatic, heteroaromatic, and other conjugated molecules, Frontier Orbitals And Reaction Paths: Selected Papers of Kenichi Fukui, World Scientific1997, pp. 33-42.

[48] M. Gaber, T.A. Fayed, M.M. El-Gamil, G.M.A. El-Reash, Structural, thermogravimetric, B3LYP and biological studies on some heterocyclic thiosemicarbazide copper (II) chelates and evaluation of their molecular docking, J. Mol. Struct. 1151 (2018) 56-72.

[49] N. Özdemir, S. Dayan, O. Dayan, M. Dinçer, N.Ö. Kalaycıoğlu. Experimental and molecular modeling investigation of (E)-N-{2-[(2-hydroxybenzylidene) amino] phenyl} benzenesulfonamide. Mol. Phys. 111(6) (2013) 707-723.

[50] R.G. Parr, L.v.Szentpaly, S. Liu, Electrophilicity index, J. Am. Chem. Soc. 121(9) (1999) 1922-1924; J.F. Janak, Proof that∂ E∂ n i= ε in density-functional theory. Phys. Rev. B 18(12) (1978) 7165-7168.

[51] P. Geerlings, F. De Proft, W. Langenaeker. Conceptual density functional theory. Chemical reviews. 103 (2003) 1793-1874; R.G. Pearson, Absolute electronegativity and hardness: applications to organic chemistry. J. Org. Chem. 54 (1989) 1423-1430.

[52] J.P. Perdew, R.G. Parr, M. Levy, J.L. Balduz Jr. Density-functional theory for fractional particle number: derivative discontinuities of the energy. Phys. Rev. Lett. 49(23) (1982) 1691-1694.

[53] G.M.A. El-Reash, O.A. El-Gammal, S.E. Ghazy, A.H. Radwan. Characterization and biological studies on Co (II), Ni (II) and Cu (II) chelates of carbohydrazones ending by pyridyl ring, Spectrochim. Acta. A. 104 (2013) 26-34.

[54] W. Linert, A. Taha. Co-ordination of solvent molecules to square-planar mixed-chalcone nickel (II) chelates: a thermodynamic and quantum-mechanical study, J. Chem. Soc. Dalton Trans. (7) (1994) 1091-1095.

[55] M.S. Masoud, A.E. Ali, M.A. Shaker, G.S. Elasala. Synthesis, computational, spectroscopic, thermal and antimicrobial activity studies on some metal–urate chelates. Spectrochimica. Acta. A. 90 (2012) 93-108.

[56] R.G. Parr, W. Yang. Density-functional theory of atoms and molecules, Oxford university press, 1989.

[57] R.G. Parr, W. Yang. Density functional approach to the frontier-electron theory of chemical reactivity. J. Am. Chem. Soc. 106 (1984) 4049-4050.

[58] P.W. Ayers, R.G. Parr. Variational principles for describing chemical reactions: the Fukui function and chemical hardness revisited. J. Am. Chem. Soc. 122 (2000) 2010-2018.

[59] J. Padmanabhan, R. Parthasarathi, V. Subramanian, P.K. Chattaraj, Electrophilicity-based charge transfer descriptor. J. Phys. Chem A. 111 (2007) 1358-1361.

[60] C. Morell, A. Grand, A. Toro-Labbe, New dual descriptor for chemical reactivity. J. Phys. Chem A. 109 (2005) 205-212.

[61] F.J. Luque, J.M. López, M. Orozco. Perspective on "Electrostatic interactions of a solute with a continuum. A direct utilization of ab initio molecular potentials for the prevision of solvent effects", Theoretical Chemistry Accounts, Springer2000, pp. 343-345.

[62] N. Okulik, A.H. Jubert, Theoretical analysis of the reactive sites of non-steroidal anti-inflammatory drugs. Internet Electron. J. Mol. Des. 4(1) (2005) 17-30.

[63] P. Politzer, P.R. Laurence, K. Jayasuriya. Molecular electrostatic potentials: an effective tool for the elucidation of biochemical phenomena. Environ. Health Perspect. 61 (1985) 191-202.

[64] M.L. Benesi, J.H. Hildebrand. A Spectrophotometric Investigation of the Interaction of Iodine with Aromatic Hydrocarbons. J. Am. Chem. Soc. 71 (1949) 2703–2707.

[65] M. Kurtomglu, M. Dagdelen, S. Toroglu. Synthesis and biological activity of novel (E, E)-vic-dioximes. Transition Met. Chem., 31 (2006)382-388.

[66] A.L. Koch, Bacterial Wall as Target for Attack.Clin. Microbiol. Rev. 16 (2003) 673-687.

[67] 67. R. Nagar. Syntheses, characterization, and microbial activity of some transition metal complexes involving potentially active O and N donor heterocyclic ligands. J. Inorg. Biochem. 40 (1990) 349-356.

[68] R.R. Zaky, T.A. Yousef, K.M. Ibrahim. Co(II), Cd(II), Hg(II) and U(VI)O_2 complexesof *o*-hydroxyacetophenone[*N*-(3-hydroxy-2-naphthoyl)] hydrazone: Physicochemical study, thermal studies and antimicrobial activity Spectrochim. Acta A. 97 (2012) 683-694.

[69] R.R.Zaky, T.A.Yousef, K.M.Ibrahim. Co(II), Cd(II), Hg(II) and U(VI)O_2 complexes of *o*-hydroxyacetophenone[*N*-(3-hydroxy-2-naphthoyl)] hydrazone: Physicochemical study, thermal studies and antimicrobial activity. Spectrochim. Acta Part A. 97 (2012) 683-694.

[70] W.T. Shier, Mammalian Cell Culture on 5 a Day: A Lab Manual of Low Cost Methods, University of the Philippines, Los Banos, 1991.

[71] N. Abdel Ghani, A.M. Mansour. Novel palladium(II) and platinum(II) chelates with 1H-benzimidazol-2-ylmethyl-N-(4-bromo-phenyl)-amine: structural studies and anticancer activity. Eur. J. Med. Chem. 47 (2012) 399-411.

[72] R. Buchtík, Z. Trávníček, J. Vančo In vitro cytotoxicity, DNA cleavage and SOD-mimic activity of copper(II) mixed-ligand quinolinonato complexes. J. Inorg. Biochem. 116 (2012) 163-171.

[73] J. Lu, Q. Sun, J. Li, L. Jiang, W. Gu, X. Liu, J. Tian, S. Yan, Two water-soluble copper(II) complexes: Synthesis, characterization, DNA cleavage, protein binding activities and in vitro anticancer activity studies. J. Inorg. Biochem. 137 (2014) 46-56.

[74] M.P.Kesavan G.G. Kumar J. Raja K. Anitha S. Karthikeyan, J. Rajesh, DNA interaction, antimicrobial, antioxidant and anticancer studies on Cu(II) complexes of Luotonin A. J. Photochem. Photobiol. B: Biology, 167 (2017) 20-28.

[75] H.H. Hammud, G.Nemer, W.Sawma, J.Touma, P.Barnabe, Y. Bou-Mouglabey, A. Ghannoum, J. El-Hajjar, J. Usta. Copper–adenine complex, a compound, with multi-biochemical targets and potential anti-cancer effect. Chemico-Biological Inter.173 (2008) 84-96.

[76] A.M. Mansour. Selective coordination ability of sulfamethazine Schiff-base ligand towards copper(II): Molecular structures, spectral and SAR study Spectrochim. Acta Part A. 123 (2014) 257-266.

[77] A. Mansour. Synthesis, spectroscopic, electrochemical, DFT and SAR studies of nifuroxazide complexes with Pd(II), Pt(II) and Ru(II). Polyhedron. 78 (2014) 10-17.

[78] J. Lu, Q. Sun, J. Li, L. Jiang, W. Gu, X. Liu, J. Tian, S. Yan. Two water-soluble copper(II) complexes: Synthesis, characterization, DNA cleavage, protein binding activities and in vitro anticancer activity studies. J. Inorg. Biochem. 137 (2014) 46-56.

Table 1. The physical and analytical data of the chalcone and its chelates.

Compound	Formulae	Color ($(\Lambda_m)^a$)	% Elemental analysis Calc. (found)					Mol. wt
			C	H	N	Metal Content		
						TGA	Atomic .absorption	
Chalcone	$C_{16}H_{16}N_2O$		76.16	6.39	11.1	----	----	252.13
C1	$C_{38}H_{45}CrN_4O_{10}$ $[CrL_2(OAc)_2].2H_2O.AcO$	Dark brown 25	59.29 (58.49)	5.89 (6.67)	7.27 (6.86)	6.75 (7.44)	6.65	769.78
C2	$C_{36}H_{42}MnN_4O_8$ $[MnL_2(OAc)_2].2H_2O$	Dark brown 14	60.59 (60.92)	5.89 (5.42)	7.84 (7.41)	7.70 (6.86)	6.83	713.98
C3	$C_{32}H_{34}CuN_6O_9$ $[CuL_2].2NO_3.H_2O$	Dark blue 179	54.12 (53.49)	5.83 (5.38)	11.83 (11.01)	8.95 (9.84)	9.5	710.19
C4	$C_{36}H_{40}ZnN_4O_7$ $[ZnL_2(OAc)_2].H_2O$	Dark brown 3	61.23 (61.04)	5.71 (5.44)	7.93 (7.6)	9.29 (9.62)	----	706.18
C5	$C_{32}H_{34}ZnCl_2N_4O_3$ $[ZnL_2Cl_2].\ H_2O$	Dark brown 1	58.33 (58.69)	5.20 (4.95)	8.53 (8.44)	9.92 (8.94)	9.87	656.13
C6	$C_{36}H_{38}CdN_4O_6$ $[CdL_2(OAc)_2]$	Dark brown 5.5	58.82 (58.10)	5.21 (5.80)	7.61 (8.11)	15.29 (14.37)	15.19	735.10

Table 2. IR spectra data (cm^{-1}) of chalcone and its chelates

No.	ν_{OH}	$\nu_{C=O}$	$\nu_{C=N}$	ν_{OAc}	ν_{M-O}	ν_{M-N}
Chalcone	--	1648	1519	--	-	-
C1	3437	1594	1530	1444 1370	520	414
C2	3435	1596	1535	1438 1369	562	427
C3	3429	1608	1568	--	550	403
C4	3424	1599	1524	1465 1377	546	417
C5	3438	1598	1555	--	596	447
C6	3435	1593	1524	1447 1372	522	425

Table 3. The Thermal amalysis data of chalcone chelates

Chelates	**Temp. ^oC**	**Mass Loss %**		**Assignment**
		Estimate	**Calc.**	
C1	28-65	4.93	4.45	Loss of lattice $2H_2O$
	113-218	8.70	8.09	Loss of lattice OAc
	218-311	15.52	15.34	Loss of coordinated 2OAc
	311-442	91.00	91.69	Dissociation of the organic chalcone with formation of Cr_2O_3+ C as final products.
C2	19-118	4.39	5.05	Loss of lattice $2H_2O$
	128-274	15.78	16.84	Loss of coordinated 2OAc
	282-491	93.14	92.30	Dissociation of the organic chalcone with formation of MnO as final products.
C3	24-75	2.79	2.53	Loss of lattice H_2O
	171-226	17.96	17.46	Loss of lattice 2 NO_3
	226-384	84.30	85.42	Dissociation of the organic chalcone with formation of CuO + 2C as final products.
C4	24-80	2.36	2.57	Loss of lattice H_2O
	116-243	16.50	16.71	Loss of coordinated 2OAc
	243-536	90.38	90.74	Dissociation of the organic chalcone with formation of Zn as final products.
C5	24-80	2.18	2.74	Loss of lattice H_2O
	161-234	10.56	10.82	Loss of coordinated Cl ions
	234-656	91.06	90.71	Dissociation of the organic chalcone with formation of ZnO as final products.
C6	87-258	16.75	16.05	Loss of coordinated 2OAc
	258-630	85.63	84.71	Dissociation of the organic chalcone with formation of CdO as final products.

Table 4. Temperatures of decomposition and activation parameters (KJmol^{-1}) of decomposition for the chelates under investigation.

Chelates	***steps***	***T(K)***	***Coast-Redfern***					
			n	***r***	***E****	***ΔH****	***-ΔS***^{a}	***ΔG****
C1	1	321.5	1	0.9870	58.64	55.97	0.225	128.44
	2	547	1	0.9714	40.12	35.58	0.137	111.01
	3	561.5	1	0.9945	88.62	83.95	0.203	198.13
	4	668.75	0	0.9931	72.23	66.67	0.056	104.74
C2	1	341.75	1	0.9789	5.70	2.86	0.073	28.06
	2	486.25	1	0.9663	23.85	19.81	0.104	70.62
	3	646	1	0.9003	32.94	27.57	0.104	95.12
C3	1	326	1	0.9904	17.49	14.78	0.104	48.74
	2	482.5	1	0.9307	72.83	68.82	0.208	169.21
	4	936.5	1	0.9511	166.25	158.46	0.140	290.01
C4	1	328.25	1	0.9928	20.94	18.21	0.108	53.85
	2	460.25	1	0.9914	42.16	38.34	0.132	99.40
	3	749.25	0	0.9912	40.05	33.82	0.004	37.11
C5	1	332.75	1	0.9929	38.72	35.95	0.159	89.10
	2	478.75	0	0.9968	44.49	40.51	0.139	107.44
	3	704.75	1	0.9397	280.44	274.58	0.362	530.35
C6	1	459.25	1	0.9911	41.44	37.62	0.145	104.52
	2	815.5	1	0.9902	323.60	316.82	0.357	608.59

[a] (KJmol^{-1} K^{-1})

Table 5. Selected bond lengths of the investigated chalcone, and its metal chelates.

Bond length ( )	**Chalcone**	**C1**	**C2**	**C3**	**C4**	**C5**	**C6**
C(13)-O(14)	1.308	1.331 1.331	1.337 1.336	1.335 1.334	1.334 1.208	1.326 1.324	1.316 1.318
C(19)-N(18)	1.374	1.396 1.392	1.397 1.399	1.398 1.396	1.394 1.387	1.387 1.389	1.386 1.387
N(18)-C(17)	1.356	1.365 1.371	1.370 1.374	1.371 1.371	1.366 1.362	1.366 1.368	1.364 1.362
M–N(18)	------	2.156 2.140	2.154 3.143	2.100 2.092	2.119 2.121	2.198 2.207	2.416 2.427
M–O(14)	------	2.051 2.084	2.067 2.117	2.067 2.040	2.120 2.140	2.179 2.186	2.401 2.402
M – OAc	------	2.126 2.130	2.141 2.153	------	2.332 2.348	------	2.554 2.552
M – Cl	------	------	------	------	------	2.585 2.589	------

Table 6. Selected bond angles of the investigated chalcone and its metal chelates.

Bond angle (^{o})	Chalcone	C1	C2	C3	C4	C5	C6
C(19)-N(18)-C(17)	120.280	119.049	119.527	119.629	120.602	120.611	120.757
		119.527	120.094	119.052	120.579	120.028	120.622
N(18)-C(19)-C(13)	120.857	113.517	113.939	114.059	115.729	115.557	116.560
		114.075	114.750	114.847	115.924	115.935	117.398
C(19)-C(13)-O(14)	116.079	114.917	116.861	115.750	117.229	118.175	118.735
		116.101	116.122	117.586	117.796	117.608	118.697
O(14)-C(13)-C(12)	116.070	116.910	115.112	115.452	116.215	116.649	118.514
		117.195	117.835	115.801	120.226	119.774	118.591
C(19)-C(13)-C(12)	127.578	128.550	125.151	127.979	126.543	125.734	122.789
		126.703	128.757	125.686	121.867	122.051	122.638
N-M-N		100.024	98.731	104.701	178.315	92.015	177.557
O-M-O		96.901	96.431	94.161	179.123	166.565	178.849
N(18)-M-O(14)	------	75.382	77.084	78.610	78.811	76.275	69.315
		76.760	92.205	161.757	101.948	92.299	109.538
		89.724	77.442	171.920	101.035	97.147	112.474
		172.326	172.551	81.053	78.219	75.921	68.669
N(18)-M-OAc	------	166.902	167.590	------	92.352	------	91.184
		91.697	88.380		87.915		91.628
		93.045	93.679		89.321		90.454
		92.755	91.719		90.412		86.623
O(14)-M-OAc	------	92.437	90.588	------	88.996	------	90.903
		169.506	169.111		91.084		93.511
		93.518	94.299		90.532		89.215
		91.532	90.576		89.385		86.399
AcO-M-OAc	------	88.526	91.167	------	179.732	------	175.387
Cl-M-Cl	------	------	------	------	------	91.485	------
Cl-M-O(14)	------	------	------	------	------	98.493	------
						94.025	
						97.275	
						88.482	
Cl-M-N(18)	------	------	------	------	------	90.372	------
						170.292	
						88.767	
						164.300	

Table 7. The calculated quantum chemical parameters of the chelates

Compound	E_{H} **(eV)**	E_{L} ***(eV)***	**(**E_{H} **-**E_{L}**) (eV)**	X ***(eV)***	**μ(eV)**	η ***(eV)***	S **(eV^{-1})**	ω***(eV)***	**Ϭ (eV)**	**ΔN_{max}(e)**
Chalcone	-4.610	-2.605	-2.005	3.608	-3.608	1.003	0.501	6.491	0.998	3.599
C1	-3.287	-2.865	-0.422	3.076	-3.076	0.211	0.106	22.421	4.739	14.578
C2	-3.269	-2.784	-0.485	3.027	-3.027	0.243	0.121	18.886	4.124	12.480
C3	-4.479	-2.814	-1.665	3.647	-3.647	0.833	0.416	7.986	1.201	4.380
C4	-4.493	-3.022	-1.471	3.758	-3.758	0.736	0.368	9.598	1.360	5.109
C5	-4.527	-3.080	-1.447	3.804	-3.804	0.724	0.362	9.998	1.382	5.257
C6	-4.519	-3.102	-1.417	3.811	-3.811	0.709	0.354	10.247	1.411	5.378

Table 8. Molecular parameters of the chalcone and its chelates

Compound	**Chalcone**	**C1**	**C2**	**C3**	**C4**	**C5**	**C6**
Sum of atomic Energies (kcal/mol)	-5.01×10^{05}	-1.35×10^{06}	-1.36×10^{06}	-1.14×10^{06}	-1.45×10^{06}	-1.74×10^{06}	-1.34×10^{06}
Kinetic Energy (kcal/mol)	-6.12×10^{03}	-1.17×10^{04}	-1.05×10^{04}	-1.12×10^{04}	-1.12×10^{04}	-9.89×10^{03}	-1.04×10^{04}
Electrostatic Energy (kcal/mol)	-8.43×10^{02}	-4.94×10^{03}	-6.18×10^{03}	-2.61×10^{03}	-5.18×10^{03}	-4.12×10^{03}	-5.93×10^{03}
Exchange-correlation Energy (kcal/mol)	1.44×10^{03}	3.71×10^{03}	3.70×10^{03}	3.06×10^{03}	3.66×10^{03}	3.11×10^{03}	3.66×10^{03}
Spin polarization (kcal/mol)	1.34×10^{03}	2.87×10^{03}	2.92×10^{03}	$2.39\times10^{0}3$	2.83×10^{03}	2.41×10^{03}	2.78×10^{03}
Total Energy (kcal/mol)	-5.05×10^{05}	-1.36×10^{06}	-1.37×10^{06}	-1.15×10^{06}	-1.46×10^{06}	-1.75×10^{06}	-1.35×10^{06}
Binding Energy (kcal/mol)	-3.94×10^{03}	-9.40×10^{03}	-9.40×10^{03}	-8.38×10^{03}	-9.32×10^{03}	-7.95×10^{03}	-9.30×10^{03}
Dipole moment (Debye)	6.98	12.56	10.41	3.87	6.55	9.14	9.63

Table 9. Ordering the nucleophilic, electrophilic and Radical attack sites for chalcone and its chelates

Compound	**Nucleophilic attack**	**Electrophilic attack**	**Radical attack**
Chalcone	O(14)>N(18)>C(16)	O(14)>C(2)>C(13)	O(14)>N(18)>C(20)
C1	C(13)>C(7)>C(9)	C(33)>C(29)>C(27)	O(50)>O(47)>C(24)
C2	O(47)>C(13)>O(50)	Mn(3)>>O(1)>O(17)	Mn(3)>>N(21)>O(17)
C3	Cu(36)>>N(18)>O(14)	N(43)>C(46)>C(42)	Cu(36)>O(14)>O(50)
C4	C(13)>O(17)>C(15)	C(27)>C(24)>C(29)	C(24)>C(26)>C(29)
C5	N(21)>N(41)>O(17)	Cl(2)>Zn(3)>N(10)	Cl(1)>Cl(2)>O(17)
C6	O(17)>C(13)>C(15)	C(27)>C(33)>O(37)	O(47)>O(50)>C(24)

Table 10.Antimicrobial activity data

Compound	**Inhibition Zone diameter(mm/mg Sample)**								
	Gram (+)bacteria	**Gram (-)bacteria**					**Fungus**		
	Staphylococcus aureus	***Escherichia Coli***	***Pseudomonas aeruginosa***	***Klebsiella pneumoniae***	***Proteus vulgaris***	***Acinetobacter***	***A. Flavus***	**Trichophyton mentagrophytes**	***Candida albicans***
Chalcone	18	17	N.D	N.D	N.D	N.D	13	N.D	16
C1	21	12	12	13	0	0	N.D	12	N.D
C2	11	12	13	10	13	0	9	0	9
C3	25	18	11	12	0	14	N.D	0	N.D
C4	21	14	10	15	0	0	N.D	0	N.D
C5	15	16	10	12	0	0	11	0	14
C6	13	12	12	13	0	0	9	0	11

N.D=Not determine

Table 11.The minimum inhibitory concentrations MIC (mg ml^{-1}) of chalcone against *C. albicans and S. aureus*

Conc	Microorganisms	
	Candidaalbicans	*Staphylococcus aureus*
0	100	100
6.25	61	66
12.5	55	29
25	29	30
50	30	30
100	29	29

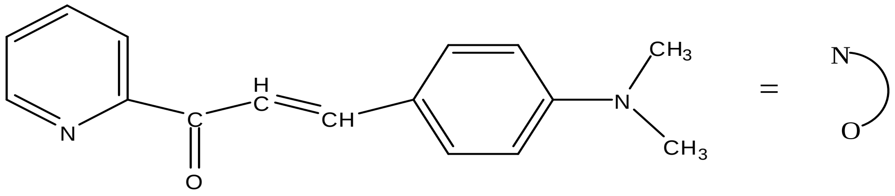

Structure 1. The structure of chalcone, (E)-3-(4-(dimethylamino)phenyl)-1-(pyridin-2-yl)prop-2-en-1-one

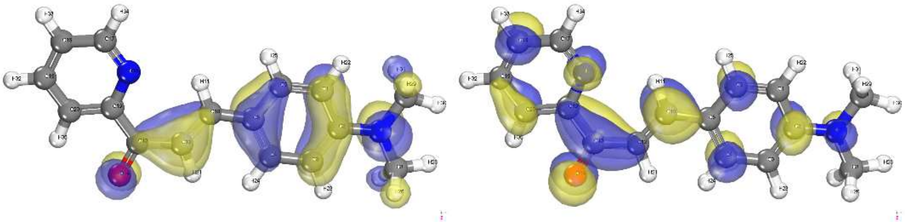

HOMO (-4.610eV) LUMO (-2.605 eV)

Figure 1.3D plots frontier orbital energies using DFT method for ligand

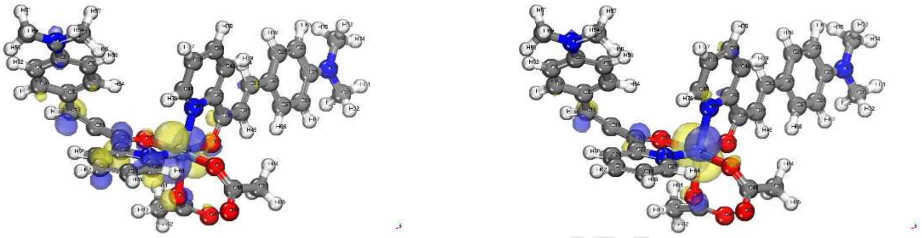

HOMO (-3.287eV) LUMO (-2.865 eV)

Figure 2.3D plots frontier orbital energies using DFT method for C1.

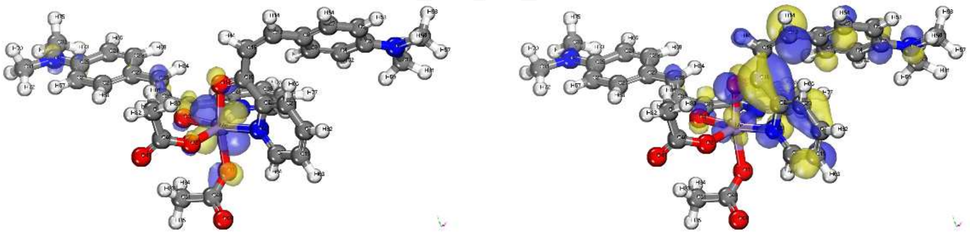

HOMO (-3.269eV) LUMO (-2.784 eV)

Figure 3.3D plots frontier orbital energies using DFT method for C2.

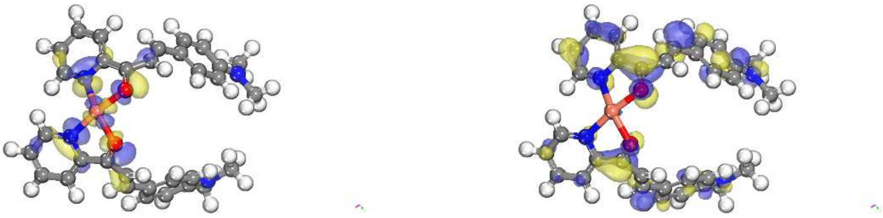

HOMO (-4.479eV) LUMO (-2.814 eV)

Figure 4.3D plots frontier orbital energies using DFT method for C3.

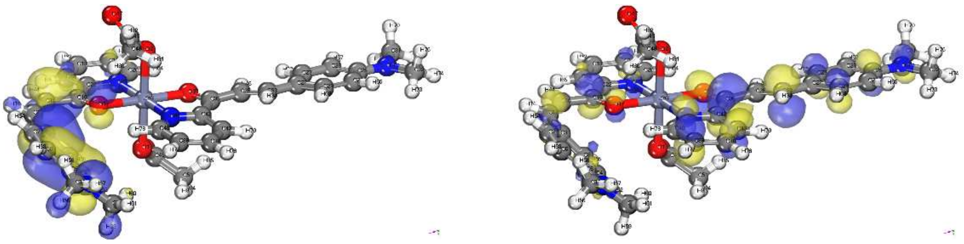

HOMO (-4.493 eV) LUMO (-3.022 eV)

Figure 5.3D plots frontier orbital energies using DFT method for C4.

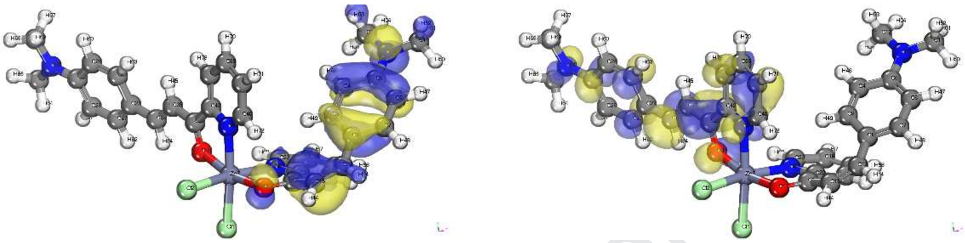

HOMO (-4.527eV) LUMO (-3.080 eV)

Figure 6.3D plots frontier orbital energies using DFT method for C5.

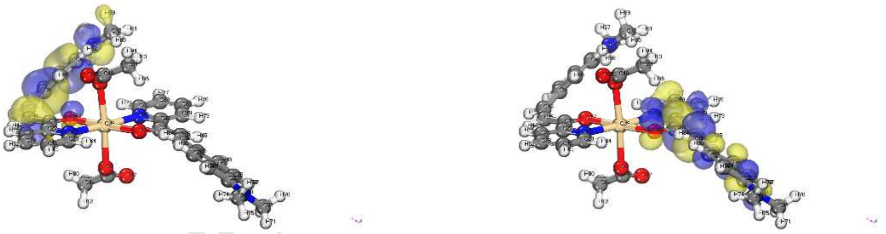

HOMO (-4.519 eV) LUMO (-3.102 eV)

Figure 7.3D plots frontier orbital energies using DFT method for C6.

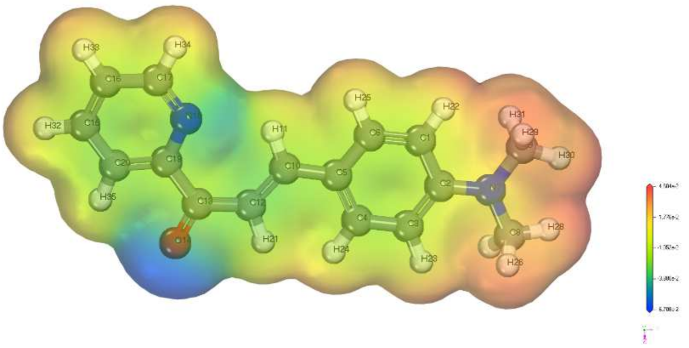

Figure 8. Molecular electrostatic potential map for ligand.

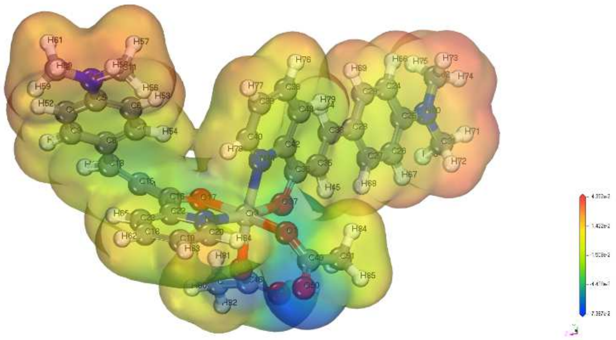

Figure 9. Molecular electrostatic potential map for C1.

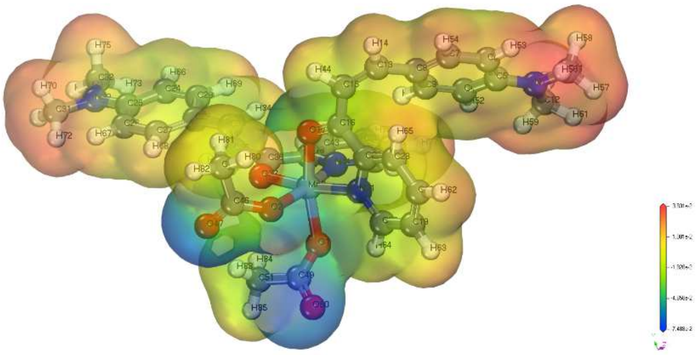

Figure 10. Molecular electrostatic potential map for C2.

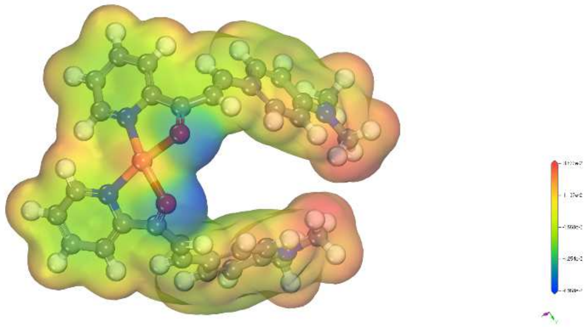

Figure11. Molecular electrostatic potential map for C3.

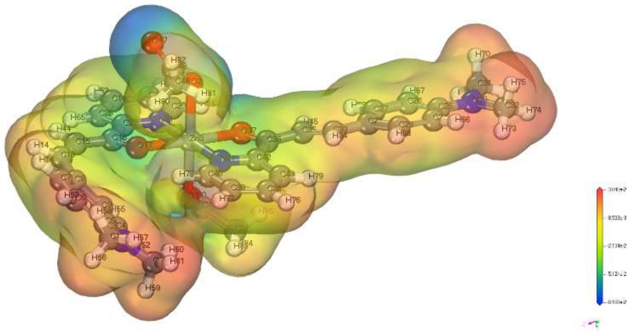

Figure 12. Molecular electrostatic potential map for C4.

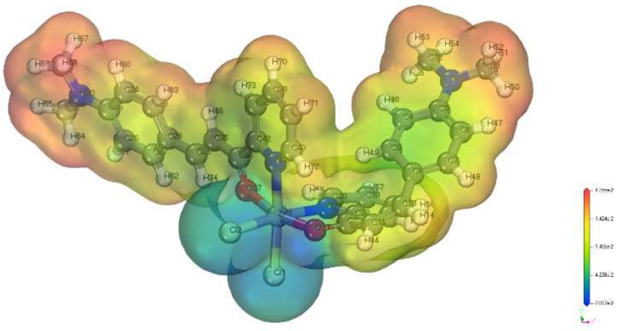

Figure 13. Molecular electrostatic potential map for C5.

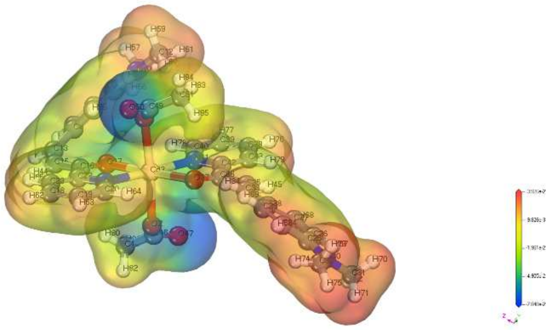

Figure 14. Molecular electrostatic potential map for C6.

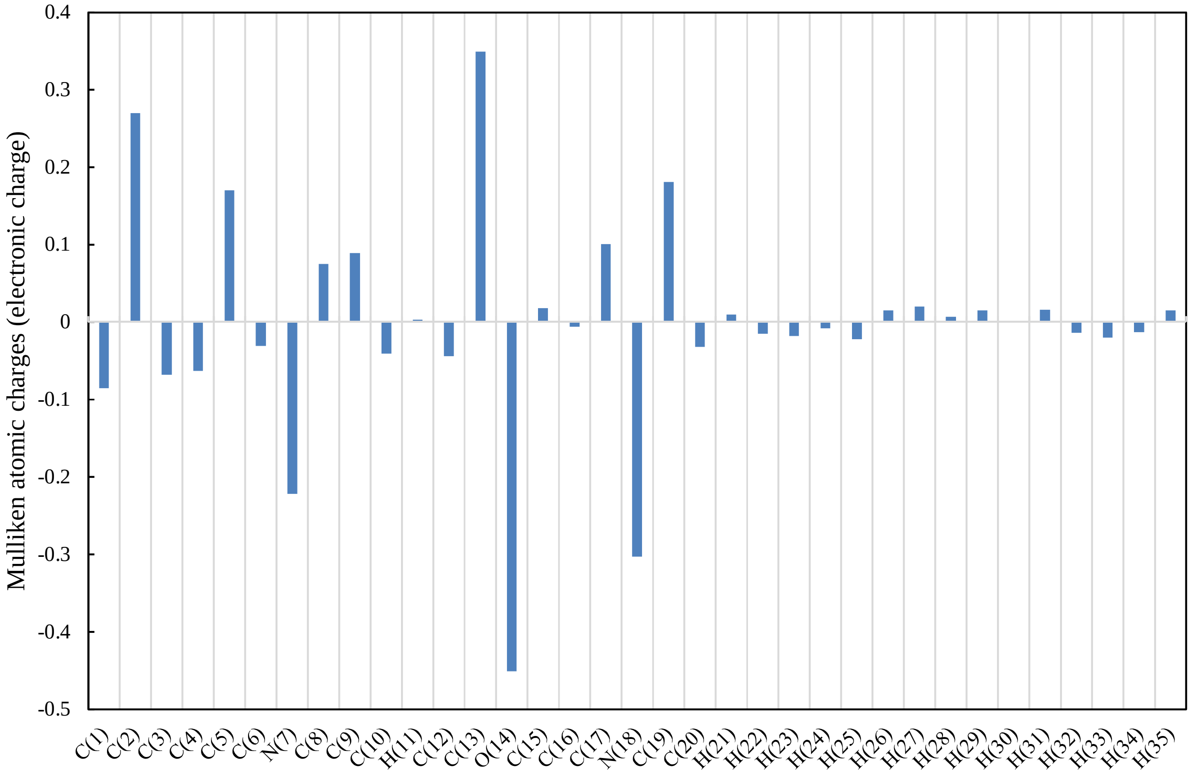

Figure 15. The Mulliken charge distribution for chalcone

Highlights

- **Synthesis and characterization of Cr(III), Mn(II), Cu(II) Zn(II) and Cd(II) chelates of (E)-3-(4-(dimethyl-amino)phenyl)-1-(pyridin-2-yl)prop-2-en-1-one by elemental and thermal analysis as well as spectral techniques (mass, IR, and electronic spectra) and magnetic measurements.**
- **Molecular orbital calculations have been performed to confirm the geometry of the isolated compounds.**
- **The in vitro antimicrobial activities of the chalcone and its metal chelates have been performed against some bacterial strains.**

Declaration of interests

√☐ The authors declare that they have no known competing financial interests or personal relationships that could have appeared to influence the work reported in this paper.

☐The authors declare the following financial interests/personal relationships which may be considered as potential competing interests:

none